

Improve Direct Torque Control of Induction Motor with Dither Injection

K Sirisha

B.Tech Scholar,

**Department of Electrical and Electronics Engineering,
Siddhardha Institute of Engineering and Technology,
Vinobha Nagar, Ibrahimpatnam, Hyderabad,
Telangana-501506, India.**

N Nireekshan

Assistant Professor,

**Department of Electrical and Electronics Engineering,
Siddhardha Institute of Engineering and Technology,
Vinobha Nagar, Ibrahimpatnam, Hyderabad,
Telangana-501506, India.**

Abstract

In this paper, a three-level inverter-fed induction motor drive operating under Direct Torque Control (DTC) is presented. A triangular wave is used as dither signal of minute amplitude (for torque hysteresis band and flux hysteresis band respectively) in the error block. This method minimizes flux and torque ripple in a three-level inverter fed induction motor drive while the dynamic performance is not affected. The optimal value of dither frequency and magnitude is found out under free running condition.

The proposed technique reduces torque ripple by 60% (peak to peak) compared to the case without dither injection, results in low acoustic noise and increases the switching frequency of the inverter. A laboratory prototype of the drive system has been developed and the simulation and experimental results are reported. Keywords. Direct torque control; dither injection; induction motor drives; three-level converter.

I. INTRODUCTION

In the middle 1980's, a simple control strategy to enhance performance of induction motor was proposed by Takahashi and Noguchi. The control strategy is popularly known as Direct Torque Control (DTC) [1]. This method gradually replacing the traditional method of Field Oriented Control (FOC) proposed by F.Blaskhe [2]. At early stages, the FOC was extensively used to established the control of AC quantities of stator flux, currents and voltages by using vector control approach.

However, this scheme is complicated due to the existence of frame transformation, current controller and requires knowledge of machine parameters. In DTC, the torque and flux are controlled independently, in which their demands are satisfied simultaneously by choosing suitable voltage vectors according to the digitized status produced from hysteresis controllers. Unlike the FOC, the torque and flux are controlled based on producing the current components (d-q axis component of stator current referring to excitation reference frame) which results in complex mathematical equations.

Despite the DTC simplicity, it is known to have two major problems, namely variable switching frequency and large torque ripple. These problems that have arisen due to the unpredictable torque and flux ρ ISSN: 2088-8694 IJPEDS Vol. 5, No. 3, February 2015 : 441 – 452 442 control behavior for various operating conditions in hysteresis operation. Obviously, many researchers have extensively proposed some/minor adjustments to minimize the problems. Space vector modulation technique is one of the popular methods to overcome the problem.

This way is widely used by researchers in order to achieve greater performance motor as was reported in [3]. The major different between DTC hysteresis based and DTC-SVM is the how to generate the stator voltage reference. In DTC-SVM, the stator voltage reference can be produced by calculating within a sampling time[4, 5].

By doing so, it can produce the constant switching as opposed the DTC-hysteresis based. However, to generate the stator voltage references involve the complex calculation and burden the processor device. Another improvement used is a variable hysteresis band. Basically, when reduce the bandwidth hysteresis band, the torque ripple has also become minimize. Even so, the possibility to select the reverse voltage vector can be occurred whenever the torque changes rapidly at the extreme conditions (i.e. at very low speeds). This mean, overshoot and undershoot of torque to vary outside the hysteresis bands might be happened. As a result, the extreme torque ripple is produced due to the inappropriate selection voltage vector. To improve the switching frequency, the dithering method is used [6, 7].

This method was applied with injecting the high switching frequency of the error component for flux and torque. However, it still also not maintains the switching frequency. Furthermore, many kinds of technique were adopted in DTC drives in order to overcome the problem as well as enhance the excellent performance of motor drives such as [8, 9]. In recent years, the researches on DTC drives utilizing multilevel inverter become the hot topic for providing the more excellent and precision of selection voltage vector to improve DTC performance[10-12]. In general, multilevel inverter can be categorized in three layouts, namely, CHMI, neutral point capacitor multilevel inverter and flying capacitor multilevel inverter as was reported [13, 14].

The all kinds of multilevel have different configurations, number of switching devices, switching states/vectors and arrangements. Multilevel inverter can offer significant advantages to improve DTC performance, especially for medium and high-power voltage application. Furthermore, it also can operate at high voltage and produce lower harmonic (i.e. slope of voltage changed dv/dt)[15]. In this paper, the DTC performances, in terms of torque ripple, harmonics distortion and switching frequency were

improved by applying appropriate selection of voltage vectors offered in CHMI topology. The selection of the appropriate vectors depends on the motor operating conditions which inherently determined by the output status of 7-level of torque hysteresis comparator. The application of simple DTC structure and fast instantaneous control with high control bandwidth offered in hysteresis based DTC can be retained. This paper is organized by section as followed; Section II described about the concept of DTChysteresis based, Section III presents the topology and switching vectors available in CHMI topology, Section IV discusses the proposed selection of vectors in DTC-CHMI; Section VI presents the simulation results to show the improvements offered and finally Section VII gives the conclusion.

II. Direct torque control algorithm

The generic DTC scheme for a three-level VSI fed IM drive is shown in figure 1. Three-level inverter voltage vectors are shown in figure 2. According to the block diagram (figure 1), the scheme includes two hysteresis band controllers. DTC is basically a stator flux oriented scheme and is based on the limit cycle control of both stator flux and torque. The stator flux controller imposes the time duration of the active voltage vectors, which move the stator flux along the reference trajectory. The torque controller determines the time duration of the zero voltage vectors, which keep the motor torque in the defined hysteresis tolerance band.

At every sampling time the voltage vector selection block chooses the inverter switching state, which reduces the instantaneous flux and torque errors. Five-level torque comparator as shown in figure 3 and two-level flux comparator are employed for three-level inverter based DTC (Behera & Das 2006). Positive torque is applied for acceleration and negative torque is applied for retardation. When the controlled torque reaches the positive lower hysteresis band, a full voltage vector is replaced with a half voltage vector.

If torque increases beyond the positive upper torque band, the zero voltage vector is applied to decrease the developed torque. For reverse rotation, in the same way, retarding voltage vectors are applied. The resulting look-up table is shown in table 1 (Behera & Das 2006).

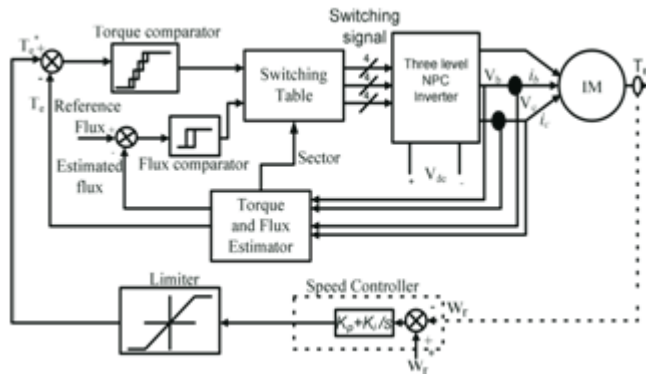


Figure 1. Block diagram of three-level inverter-fed DTC induction motor drive.

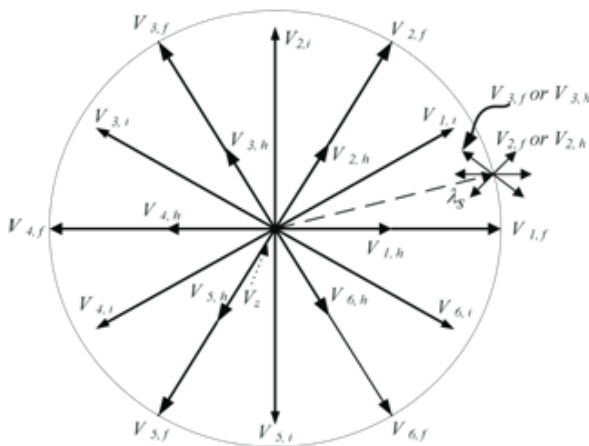


Fig.2. Output voltage vector of three-level VSI.

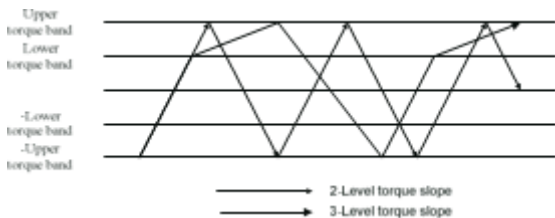


Fig.3. Torque slope pattern of three-level inverter

Due to introduction of delay in a practical system, it is found that the switching frequencies of the power switches are reduced.

An analytical study has been carried out for switching frequency under different hysteresis band conditions and the analysis is shown in figure 4. Further, digital implementation of hysteresis controllers for torque and flux introduces delay in the program execution. This leads to increase in current, torque and flux ripples, and gives rise to acoustic noise.

Table 1. Switching look-up table.

λ_s is	Torque	
sector k	↑	↓
Flux	$V_{k+1,h}$	$V_{k+1,f}$
↑	$V_{k+1,h}$	V_z
↓	$V_{k+2,h}$	$V_{k+2,f}$

↑ increase, ↑ more increase and ↓ decrease

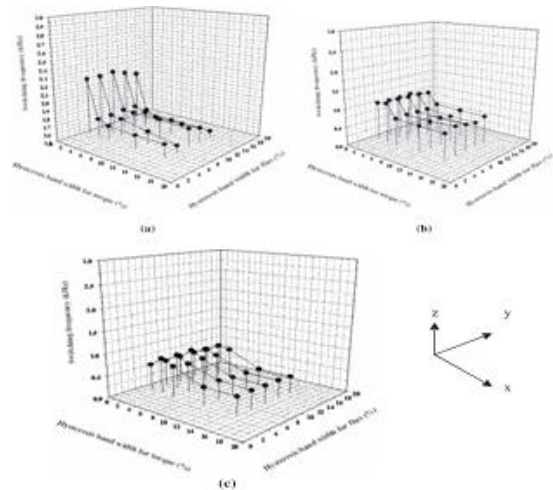


Figure4. Analytical results of convention aDTC. z-axis: Switching frequency in kHz. x-axis: Torque hysteresis band in %. y-axis: Flux hysteresis band in %. (a) No delay in the feedback loops; (b) 10µs delay in the feedback loops; (c) 20µs delay in the feedback loops.

The developed torque is not constrained within the error band of the hysteresis controller (Ambrozic et al 2004). To overcome the difficulty as mentioned, a compensating technique is developed, which is based on the injection of high frequency triangular dither signal. The inverter switching frequency is analysed for zero time delay, 10µs and 20µs in the estimator block in the feedback path.

Figures 4a–c show the simulation results of the average switching frequency against the torque and flux hysteresis band width when the motor is operating under freerunning condition with a speed of 955 rpm. In these figures, the hysteresis bandwidths are normalized with respect to the rated stator flux amplitude and rated torque respectively. From the above figures, it is confirmed that the inverter switching frequency mainly depends on torque hysteresis band width. It is observed that the switching frequency cannot be raised, although hysteresis bandwidth for torque control is reduced to a sufficiently low value (Ambrozic et al 2004). This is due to band constrain of the DTC drive.

When $10\mu\text{s}$ delay is introduced in the feedback path, the upper limit of switching frequency is nearly 1.1 kHz. For a delay of $20\mu\text{s}$ the switching frequency becomes 0.8 kHz. The switching frequency, however, is somewhat decreased when the hysteresis bandwidths are excessively diminished. This is because of abnormal resonant oscillations between the flux and torque ripples and the dither signals. As the hysteresis bandwidths are decreased, the gradient of the flux error and the torque error with respect to time becomes closer to that of the dither signals. This causes the inappropriate switching in the hysteresis elements, which results in the non-optimized PWM pattern (Noguchi et al 1999).

III. Analytical study of dither signal injection

Dither injection is required to reduce torque and flux ripple of the conventional DTC drive as mentioned in § 2 in the presence of measurement and computational delays. The sensors used for the present system are (LV-25 P) for voltage measurement and (LA 55-P) for current measurement respectively. The delays associated with these sensors are due to sensor response time. A/D conversion time is $2\mu\text{s}$ for multiplexed channel and 800 ns for parallel channel. Execution time of the estimator is around $1.66\mu\text{s}$. So average delay associated with the DTC drive is around $7.5\mu\text{s}$.

The presence of delay leads to low switching inverter frequency which is corrected by dither injection. Figures 5a–b show the schematic diagram of the dither injected system, where triangular waves are employed as the dither signals in the error blocks. The dither signal is superimposed on the torque and flux error loop, so that the overall system performance can be improved. The frequency of the triangular waves should be approximately 30 kHz to keep the three-level NPC inverter switching frequency more than 5 kHz and their amplitudes should be small compared to the hysteresis band for the flux and torque error band. However, it is not necessary to fix

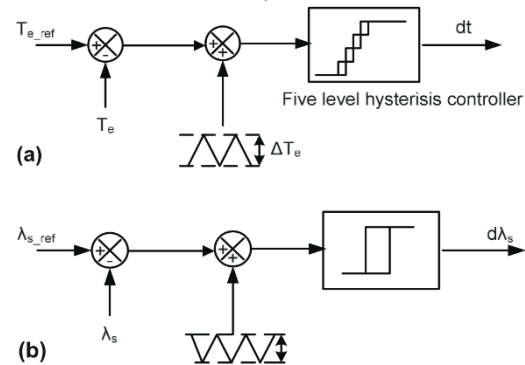


Figure 5. (a) Injection of triangular dither in torque control loop; (b) Injection of triangular dither in flux control loop.

Specifically the relative phase between the two dither signals because the frequency spectra of the current and the acoustic noise of the motor can be dispersed (Noguchi et al 1999). The inverter switching frequency is a function of the hysteresis band for the torque control. Since the relay operation of the torque control is performed alternatively between one of the zero-voltage vectors and one of the non zero-voltage vectors, only one inverter leg of the three phases changes its own switching state at every switching time of the hysteresis element. This implies that the averaged inverter switching frequency can be approximated to one-sixth of the dither frequency for the three-level NPC inverter-fed induction motor drive. In the conventional switching algorithm, applied voltage vector can be selected based on the condition of the flux and torque error command.

But due to inherent delay in the feedback system, the torque and flux errors will cross the boundary of flux and torque error band limits. This phenomenon is clearly explained in Ambrozic et al (2004). Using the present method, the flux and torque ripples can be suppressed less than the hysteresis band limit, and the switching cycles of the hysteresis elements are increased accordingly. The hysteresis bands of the relay elements act inherently as insensitive bands, but, owing to the superposition of the triangular waves on the errors, the hysteresis elements can change their switching states, regardless of the minute error variations. It should be noted that the dynamic response of the original system is not degraded.

IV. Analysis and comparison of results

The simulation is carried out in Matlab-Simulink and typical results are reported here. Figures 6–8 show the computer simulation results that have been obtained by driving the induction motor at 1000 rpm under the free running condition. The rated values and the nominal parameters of the motor are shown in table 2. This simulation result is obtained under rated flux condition. All simulations have been carried out without and with triangular dither injections for comparison. Triangular dither is injected here having a frequency of 30 kHz. Amplitude of dither signal in torque control loop is 5% of rated torque and the amplitude dither signal in flux control loop is 5% of reference flux. Both the dither signals are opposite to each other in phase to minimize the acoustic noise (Kinkaid et al 2002).

Table 2. Induction motor drive ratings and parameters.

(Referred to stator)	
DC link capacitor $C_1 = C_2$	2200 μ F
Power	5 hp
Voltage ($L - L$)	415 V
Current	7.6 A
Frequency	50 Hz
Rated torque	24.5 N-m
Speed	1440 rpm
Stator resistance (R_s)	2.177 Ω
Rotor resistance (R_r)	1.275 Ω
Stator leakage inductance (L_{ls})	0.0081 H
Rotor leakage inductance (L_{lr})	0.0081 H
Mutual inductance between stator and rotor (L_m)	0.1683 H

Improved direct torque control of induction motor with dither injection

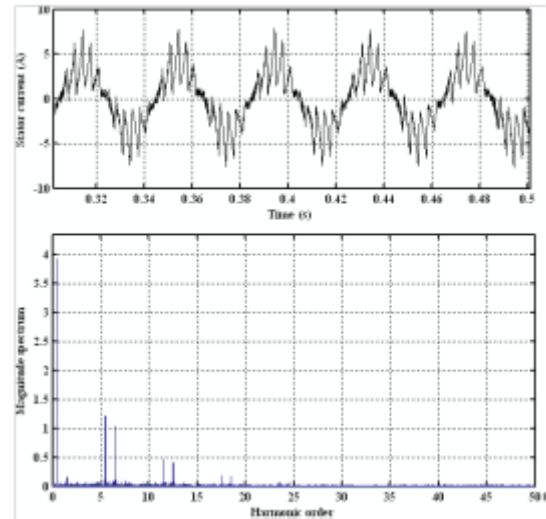


Figure 6a. Steady state stator current and harmonic spectrum without dither injection.

Figures 6a and b show the three-phase steady state stator current and its harmonic spectrum without and with dither injection respectively. From the simulation result, it is confirmed that the current ripple is reduced due to dither injection in the flux loop. The harmonic

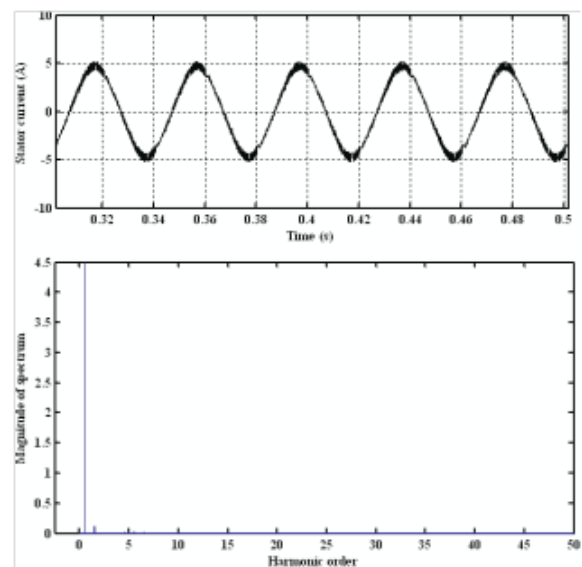


Figure 6b. Steady state stator current and harmonic spectrum with dither injection.

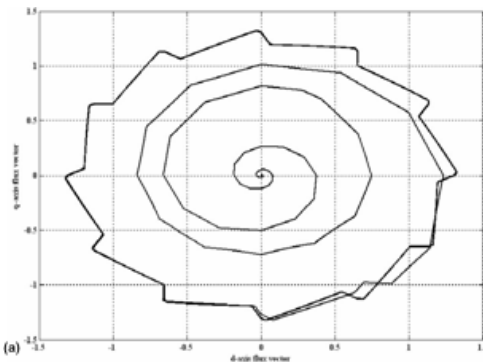


Figure 7a. Stator flux trajectory without dither injection.

Spectrum also improved. Figure 7a and b show the stator flux trajectory without and with dither injection respectively. A $7.5\mu s$ delay in the feedback path is considered. This shows that the flux error band crosses the boundary of flux error limit without dither injection. This increases flux ripple so also current ripple. A smoother flux trajectory is achieved by injection of triangular dither.

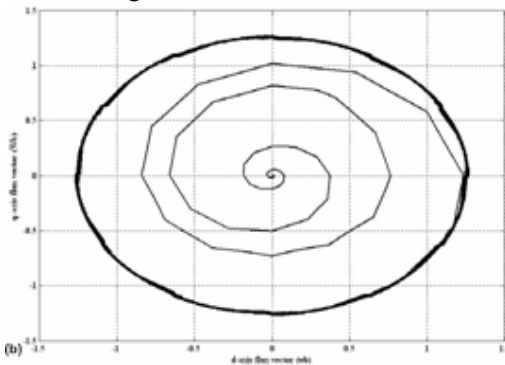


Figure 7b. Stator flux trajectory with dither injection.

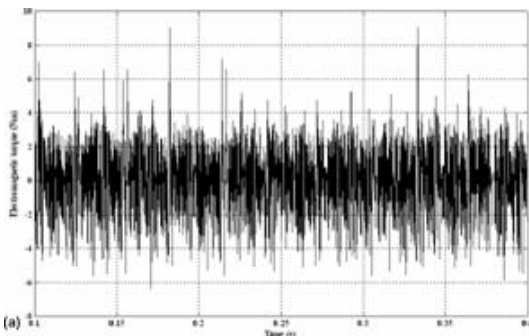


Figure 8a. Electromagnetic torque without dither injection.

Figure 8 shows the simulation results of the developed electromagnetic torque with and without dither injections. According to the figure, when dithering is applied to the system the peak to peak torque ripple is reduced by 60% compared to that of the system when no dither is injected. To show the effectiveness of the triangular dither injection on inverter switching frequency, computer simulation study has also been carried out. Figures 9a and b show the instantaneous switching frequency without and with dither injections. It is clearly seen that inverter switching frequency increases to an average switching frequency of 2.2kHz. This leads to improvement in current and torque ripple. The three-phase three-level inverter consists of six dual IGBT modules (SEMIKRON, SKM 75GB128D, 1200V, 100A), i.e. two IGBTs per module is used in this topology. Three

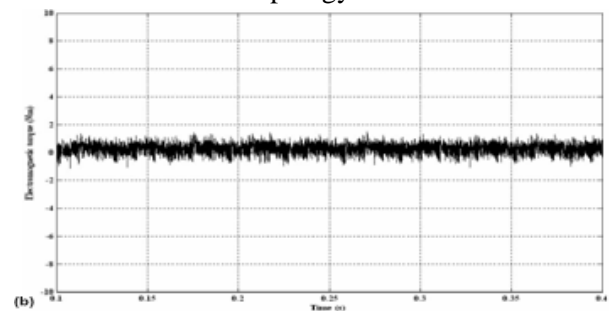


Figure 8b. Electromagnetic torque with dither injection.

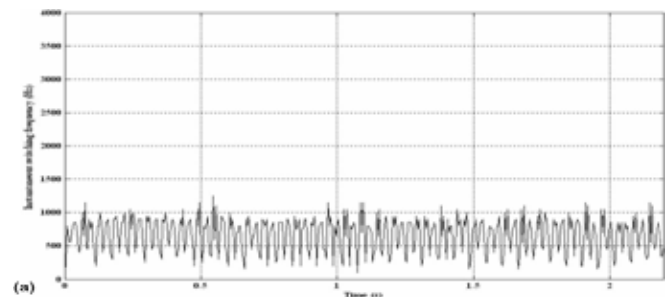


Figure 9a. Instantaneous switching frequency without dither signal.

IGBTs with feedback diodes are used as clamping diode to match the characteristics of the IGBT module. The rectifier is connected to capacitors and each capacitor rating is $2200\mu F$, 400V DC.

The DTC drive along with all its components are implemented by using a DSP based DS1104 PCI dSPACE board. Induction motor ratings and parameters are given in table 2. Triangular dither is obtained using repetitive block of Matlab-Simulink. For experimental set-up this triangular signal is generated by the DSP. Figures 10a and b show the torque and speed profile without and with triangular dither injections respectively. The electromagnetic torque is measured using system model. From

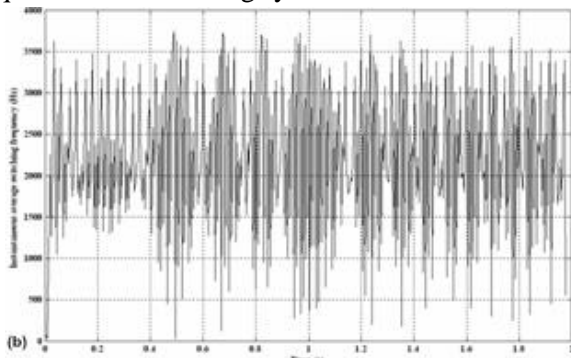


Figure 9b. Instantaneous switching frequency with triangular dither signal of 30kHz.

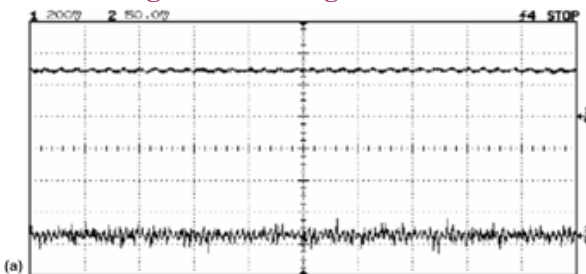


Figure 10a. Speed and electromagnetic torque when dither is not applied. Ref: 1: Speed: 500rpm/div; Ref: 2: Electromagnetic torque: 0.5N-m/div.

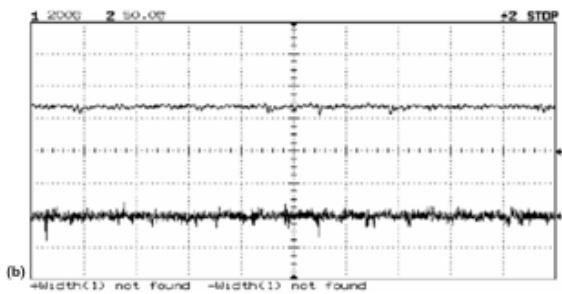


Figure 10b. Speed and electromagnetic torque when dither is applied. Ref: 1: Speed: 500rpm/div; Ref: 2: Electromagnetic torque: 0.5N-m/div.

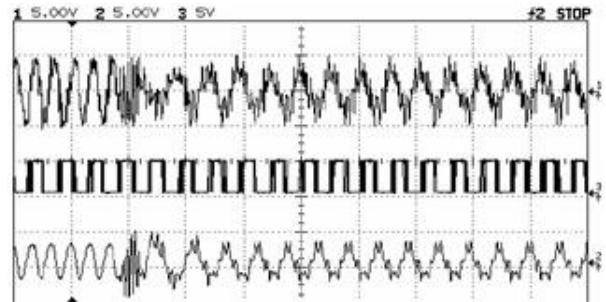


Figure 11. Transition from dither injection to without dither injection. Ref: 1: Line-to-line stator voltage; Ref: 2: Stator current (5A/div); Ref: 3: Switching pulse.

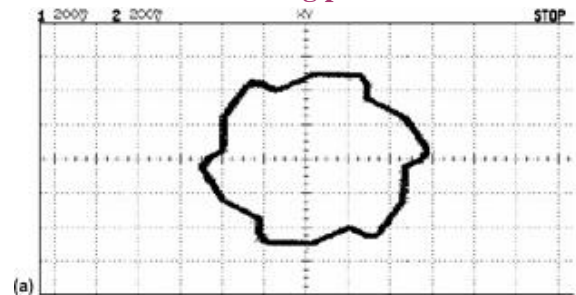


Figure 12a. Steady state stator d – q axis flux locus without dither injection.

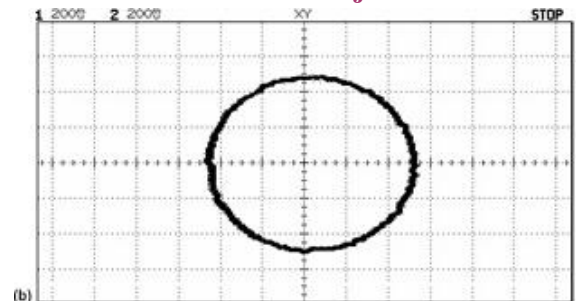


Figure 12b. Steady state stator d – q axis flux locus with triangular dither injection.

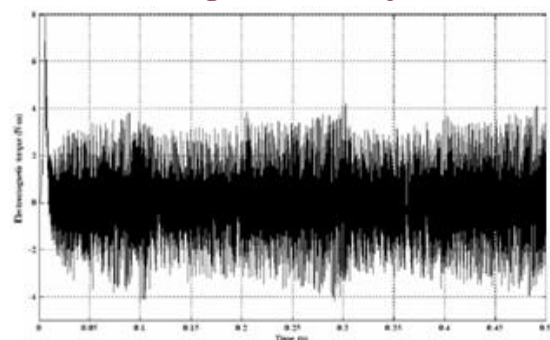


Figure 13. Electromagnetic torque when dither is not applied and induction motor is operating at low speed.

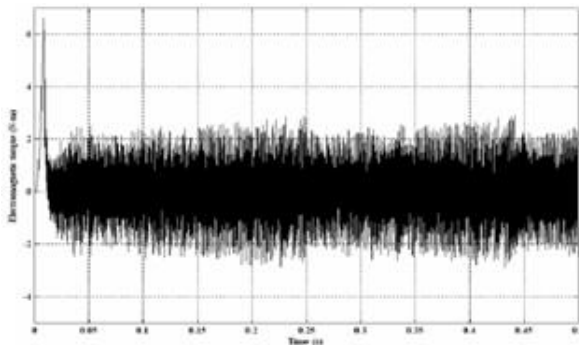


Figure 14. Electromagnetic torque when dither is applied and induction motor is operating at low speed.

The above-mentioned figures, it is observed that the torque ripple and speed fluctuations are minimized using dither injection. In the DTC scheme given in figure 1, dither signal is applied for 4 seconds, and then the dither signal is removed. The resultant experimental result is given in figure 11. Figures 12a and b show the stator flux trajectory without dither and with triangular dither injection. It is observed that the flux ripple is also reduced using dither signal injection. In classical DTC methods, torque ripples are normally pronounced under starting and low speed conditions. Dither injection also improves the low speed performance of the DTC IM drive. When the induction motor is running at 50rpm without dither injection, the electromagnetic torque ripple increases as shown in figure 13. However, by injecting triangular dither signal the torque ripple is reduced and it is confirmed from simulation result given in figure 14.

V. Conclusion

This paper has presented the torque ripple reduction with dithering technique. The proposed method successfully reduces the torque ripple. The MATLAB results presented for the torque ripple reduction. The simulated waveforms are presented to validate the claim of torque ripple reduction. The current waveforms are also presented to support the superiority of the proposed DTC method. The torque ripple reduction are observed around 30%.

REFERENCES

- [1] Takahashi, I. and T. Noguchi, A New Quick-Response and High-Efficiency Control Strategy of an Induction Motor. *Industry Applications, IEEE Transactions on*, 1986. IA-22(5): p. 820-827.
- [2] Ohtani, T., N. Takada, and K. Tanaka. Vector control of induction motor without shaft encoder. In *Industry Applications Society Annual Meeting, 1989., Conference Record of the 1989 IEEE*. 1989.
- [3] Jun-Koo, K. and S. Seung-Ki. Torque ripple minimization strategy for direct torque control of production motor. In *Industry Applications Conference, 1998. Thirty-Third IAS Annual Meeting. The 1998 IEEE*. 1998.
- [4] Casadei, D., G. Serra, and A. Tani. Improvement of direct torque control performance by using a discrete SVM technique. in *Power Electronics Specialists Conference, 1998. PESC 98 Record. 29th Annual IEEE*. 1998.
- [5] Tripathi, A., A.M. Khambadkone, and S.K. Panda, Torque ripple analysis and dynamic performance of a space vector modulation based control method for AC-drives. *Power Electronics, IEEE Transactions on*, 2005. 20(2): p.485-492.
- [6]Noguchi, T., et al., Enlarging switching frequency in direct torque-controlled inverter by means of dithering. *Industry Applications, IEEE Transactions on*, 1999. 35(6): p. 1358-1366.
- [7] Behera, R.K. and S.P. Das. High performance induction motor drive: A dither injection technique.in *Energy, Automation, and Signal (ICEAS), 2011 International Conference on*. 2011.
- [8] Bird, I.G. and H. Zelaya-De La Parra, Fuzzy logic torque ripple reduction for DTC based AC drives. *Electronics Letters*, 1997. 33(17): p. 1501-1502.

[9] Sutikno, T., et al., An Improved FPGA Implementation of Direct Torque Control for Induction Machines. *Industrial Informatics, IEEE Transactions on*, 2013. 9(3): p. 1280-1290.

[10] Ahmadi, M.Z.R.Z., et al. Improved performance of Direct Torque Control of induction machine utilizing 3-level Cascade H-Bridge Multilevel Inverter. in *Electrical Machines and Systems (ICEMS), 2013 International Conference on*. 2013.

[11] Ahmadi, M.Z.R.Z., et al. Minimization of torque ripple utilizing by 3-L CHMI in DTC. in *Power Engineering and Optimization Conference (PEOCO), 2013 IEEE 7th International*. 2013.

[12] Alloui, H., A. Berkani, and H. Rezine. A three level NPC inverter with neutral point voltage balancing for induction motors Direct Torque Control. in *Electrical Machines (ICEM), 2010 XIX International Conference on*. 2010.

[13] Nabae, A., I. Takahashi, and H. Akagi, A New Neutral-Point-Clamped PWM Inverter. *Industry Applications, IEEE Transactions on*, 1981. IA-17(5): p. 518-523.

[14] Malinowski, M., et al., A Survey on Cascaded Multilevel Inverters. *Industrial Electronics, IEEE Transactions on*, 2010. 57(7): p. 2197-2206.

[15] Ahmadi, M.Z.R.Z., et al. High efficiency of switching strategy utilizing cascaded H-bridge multilevel inverter for high-performance DTC of induction machine. in *Energy Conversion (CENCON), 2014 IEEE Conference on*. 2014.